Geochemical Journal, Vol. 40, pp. 135 to 148, 2006

Multiple records from osmium, neodymium, and strontium isotope systems of the Nikubuchi ultramafic complex in the Sambagawa metamorphic belt, central Shikoku, Japan

RYOKO SENDA,[1]* TAKUYA KACHI[2] and TSUYOSHI TANAKA[3]

[1]Center for Chronological Research, Nagoya University, Furo-cho, Chikusa-ku, Nagoya 464-8602, Japan
[2]Department of Earth and Planetary Sciences, Graduate School of Science, Nagoya University, Furo-cho, Chikusa-ku, Nagoya 464-8602, Japan
[3]Department of Earth and Environmental Sciences, Graduate School of Environmental Studies, Nagoya University, Furo-cho, Chikusa-ku, Nagoya 464-8601, Japan

(*Received December 19, 2004; Accepted September 1, 2005*)

The isotopic compositions of Os, Nd, and Sr, as well as major elements of dunites, spinel lherzolites, websterite, and serpentinite from the Nikubuchi ultramafic cumulous complex in the Sambagawa metamorphic belt (SMB) were investigated. The Nikubuchi ultramafic complex is a layered cumulate and is surrounded by a metagabbro massif in the SMB. We obtained a Sm-Nd whole-rock isochron of the Nikubuchi complex with an age of 138 ± 18 (2σ) Ma and an initial $^{143}Nd/^{144}Nd$ ratio of 0.51270 ± 3. The Nikubuchi complex contains well preserved protogranular textures and cumulous layering structures, and has good correlation coefficients among the major element abundances, which indicate an event before the Sambagawa metamorphism. The ε_{Nd} values of 138 Ma (+3.5 to +5.3) correspond to the isotope signatures of ocean island basalt (OIB) or island arc basalt (IAB), and not mid-ocean ridge basalt (MORB). Taking the results of previous studies into consideration, the most likely origin of the Nikubuchi complex is that of a fragmented block of residual cumulate formed by the OIB magma chamber. The Rb-Sr isotope system has been disturbed by hydration and/or metamorphism after 138 Ma, and the Re-Os isotope system also has no valid isochron. One of the possible causes is that rhenium addition by hydration has occurred subsequent to 60 Ma. The results of the isotope systems show that hydration can cause disturbance in Re-Os systems but not in Sm-Nd systems. This probably reflects differences between these systems in resistance of the host phase.

Keywords: ultramafic complex, Re-Os isotope system, Sm-Nd isotope system, Sambagawa metamorphic belt, cumulate complex

INTRODUCTION

Subduction zones are active regions where the crust is recycled into the mantle. Magmatism in a subduction zone involves both mixing and differentiation processes, with the subducted plates producing the mantle's elemental and isotopic heterogeneity. In subduction zones, various materials, including oceanic sediments, continental clastics, and oceanic volcanics, are gathered and recycled into the inner earth as subducting materials. The Japanese islands form an island arc along the subduction zone at the western margin of the Pacific Ocean. In the southern part of southwest Japan, the Philippine Sea plate is subducting at the Nankai trough. Many clastics from the Japanese islands are transported into the trench and accrete on its landward side. The accretion and recycling of clastics and oceanic crust cannot be observed directly where they occur, because these processes take place deep beneath the surface. The Sambagawa metamorphic belt (SMB) is an ancient accretionary prism, which is presently emplaced at the earth's surface. Therefore, the SMB affords the opportunity to investigate the detailed processes of accretion and recycling in a subduction zone. There are many uplifted subduction materials present in historical accretions in southwest Japan; the SMB is located at the northern margin of the outer zone of southwest Japan, extending from eastern Kyushu to Kanto (Fig. 1a). The SMB underwent a high pressure-low temperature (P-T)-type metamorphism along the eastern edge of the Eurasian continent during the Mesozoic (e.g., Miyashiro, 1961). At the Besshi area in central Shikoku, many ultramafic and mafic rocks are exposed (Takasu, 1984a; Kunugiza *et al.*, 1986); the area has experienced

*Corresponding author (e-mail: rsenda@jamstec.go.jp)
*Present address: Institute for Research on Earth Evolution, Japan Agency for Marine-Earth Science and Technology, 2-15 Natsushima-cho, Yokosuka 237-0061, Japan.

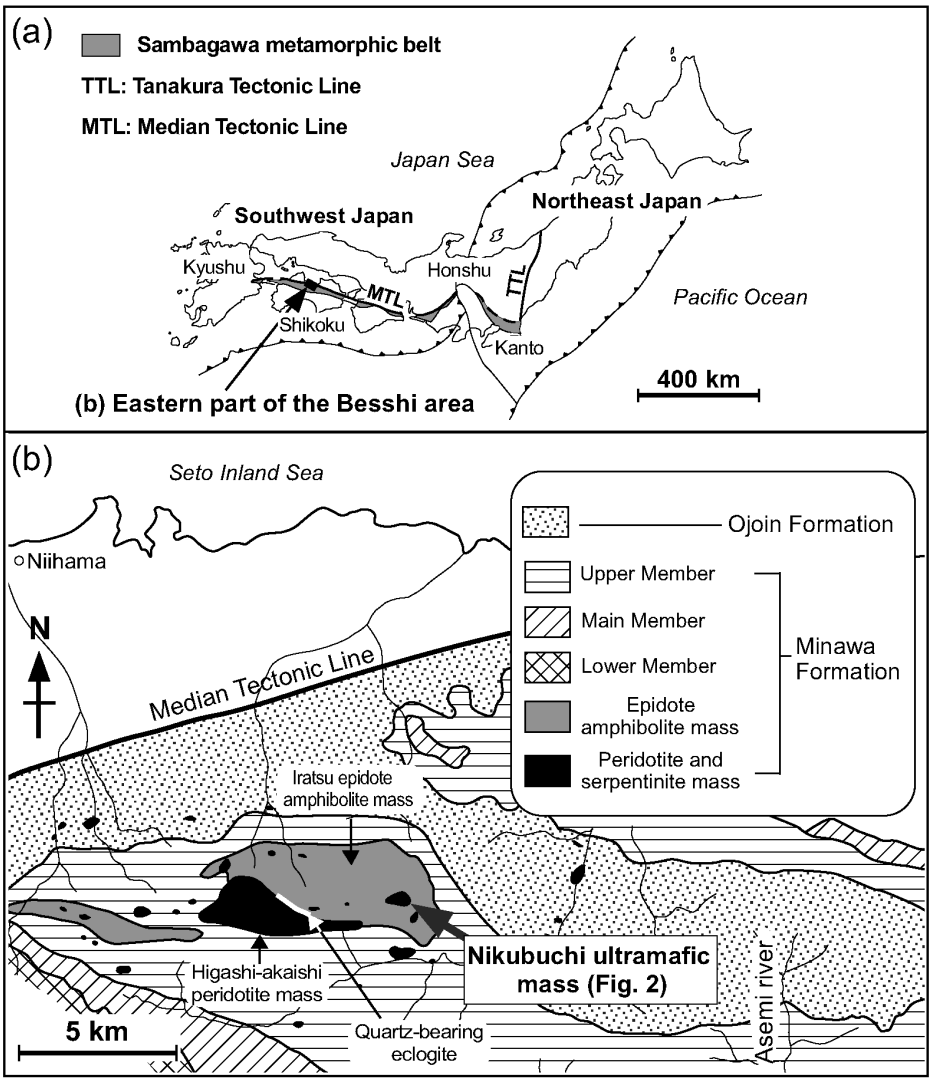

Fig. 1. (a) Distribution of the Sambagawa metamorphic belt and the location of the eastern part of the Besshi area. (b) Geological map of the eastern part of the Besshi area and the location of the Nikubuchi ultramafic complex and surroundings (modified from Kunugiza, 1984)

higher metamorphic pressures and temperatures than other areas of the SMB (Higashino, 1975; Enami, 1982).

The origin and histories of these ultramafic rocks provide important information that assists in clarifying material recycling in the mantle wedge or additional process in the subduction zone. The geochemical characteristics of the ultramafic rocks illustrate how they differ in character from the sedimentary rocks that are the main components of the accretionary prism, and can contribute to clarification of the origin and behavior of the accretionary prism in subduction systems. In particular, isotopic data are expected to reveal information on the origin and history of these rocks (e.g., Reisberg and Zindler, 1986; Reisberg *et al*., 1989; Burnham *et al*., 1998; Puchtel *et al*., 1999). The Nikubuchi ultramafic complex exhibits clear igneous layering in the Besshi area. We examined Os, Nd, and Sr isotope ratios as well as major and trace element compositions of this complex.

Geological Setting and Samples

The Japanese islands consist largely of post-Paleozoic accretionary prisms that have developed continuously along the eastern margin of the Eurasian continent. The Tanakura Tectonic Line separates northeast and southwest Japan; the latter is subdivided into inner and outer zones by the Median Tectonic Line, which strikes approximately E-W and is more than 1000 km long (Fig. 1a). The outer zone is composed mainly of three geologic belts, the northernmost of which is the SMB. In central Shikoku,

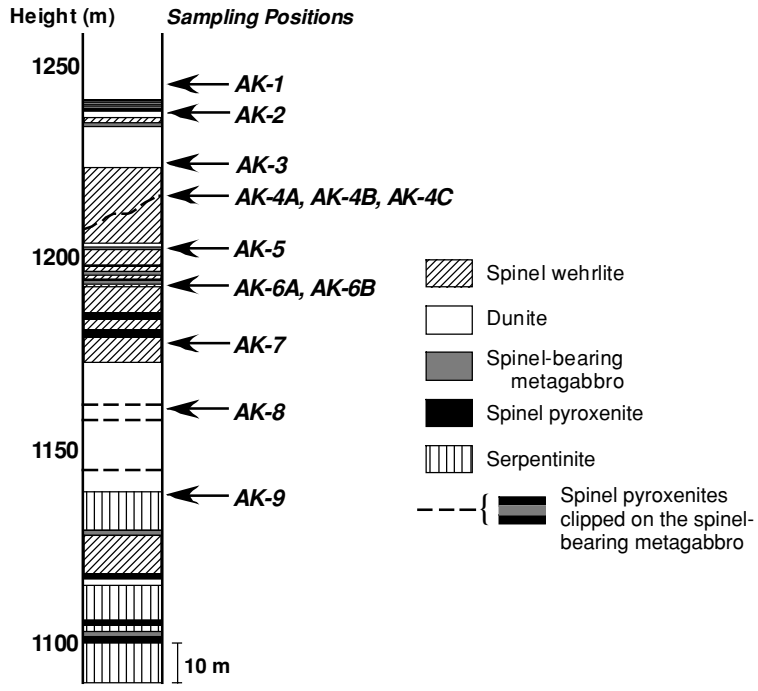

Fig. 2. Columnar section of the Nikubuchi ultramafic complex and sampling points (modified from Yokoyama, 1980).

the SMB is further subdivided into the Besshi and Oboke tectonic units (Takasu and Dallmeyer, 1990). The Besshi unit is dominated by pelitic, basic, and siliceous schists. The metamorphic age of the unit is considered to be Late Cretaceous (100–120 Ma) on the basis of a Rb-Sr whole-rock isochron age of 116 ± 10 Ma for pelitic schists (Minamishin *et al*., 1979), U-Pb ages ranging from 112 to 132 Ma on overgrown parts of zircons in quartz eclogite (Okamoto *et al*., 2004), the $^{40}Ar/^{39}Ar$ whole-rock ages of schists that range between 85 and 94 Ma (Takasu and Dallmeyer, 1990) and the muscovite K-Ar age of schists, which range from 65 to 90 Ma (Itaya and Takasugi, 1988).

In the eastern part of the Besshi area, in central Shikoku, the rocks are stratigraphically divided into the Minawa and Ojoin Formations (Kojima *et al*., 1956) (Fig. 1b). The Minawa Formation is composed mainly of pelitic, siliceous, and basic schist. The upper member of the Minawa Formation is composed predominantly of alternating beds of pelitic schist and greenschist, with some ultramafic and metagabbro bodies, including for example the Higashiakaishi peridotite mass, Iratsu epidote-amphibolite mass, and Nikubuchi ultramafic complex (Takasu, 1984b, 1989; Kunugiza *et al*., 1986).

The Nikubuchi ultramafic complex (Nikubuchi complex) is about 500 × 200 m^2 in area. It forms a layered structure composed mainly of dunite, wehrlite, and spinel pyroxenite (Fig. 2; Yokoyama, 1980). The Nikubuchi complex is surrounded by the Eastern Iratsu epidote amphibolite mass, which originated from layered gabbro (Banno *et al*., 1976). The relationship between the Nikubuchi complex and its surroundings is unclear. Petrological studies of the Nikubuchi complex were carried out by Yokoyama and Mori (1975), Yokoyama (1976, 1980), and Kunugiza (1984). Their studies suggest that the Nikubuchi complex is a magmatic cumulate that originated in the upper part of the mantle. Evidence for this includes Fe^{3+} and Ti-rich Cr-spinel, low Mg/Fe ratios in clinopyroxene, and the complex banded structures in the wehrlite and metagabbro. This cumulate first recrystallized under granulite facies conditions (750°C, 0.5–1.0 GPa; Yokoyama, 1980) in the lower crust, and then underwent epidote-amphibolite facies conditions (Sambagawa metamorphism, 600°C, 0.8–1.3 GPa; Yokoyama, 1980).

The lithology of the Nikubuchi complex changes gradually, as the columnar section illustrates (Fig. 2). For example, lherzolite usually occurs at boundaries between wehrlite and spinel pyroxenite (Yokoyama, 1980). We conducted Os, Nd, and Sr isotope analyses on 12 samples to clarify the origin of the Nikubuchi complex. Five dunites (samples AK-1, -2, -3, -6A, and -8) and five spinel lherzolites (AK-4A, -4B, -4C, -5, and -6B) were analyzed as well as one websterite (AK-7) and one serpentinite (AK-9).

The mineral assemblages of analyzed samples are shown in Table 1. Each thin section has a granular tex-

Table 1. The mineral assemblages of the Nikubuchi ultramafic rocks

		Ol	Cpx	Opx	Spl	Retrograde minerals
AK-1	dunite	◎	△	—	—	serpentinite + magnetite+ chlorite + carbonate
AK-2	dunite	◎	△	—	—	serpentinite + magnetite + chlorite + talc
AK-3	dunite	◎	○	○	△	serpentinite + magnetite + chlorite + talc
AK-4A	spinel lherzolite	◎	◎	◎	△	serpentinite + magnetite + chlorite + talc
AK-4B	spinel lherzolite	◎	◎	◎	△	serpentinite + magnetite + chlorite + talc
AK-4C	spinel lherzolite	◎	◎	◎	△	serpentinite + magnetite + chlorite + talc
AK-5	spinel lherzolite	◎	○	○	△	serpentinite + magnetite + talc
AK-6A	dunite	◎	△	△	△	serpentinite + magnetite + chlorite + talc
AK-6B	spinel lherzolite	◎	◎	◎	△	serpentinite + magnetite
AK-7	websterite	—	◎	◎	△	serpentinite
AK-8	dunite	◎	△	—	△	serpentinite + magnetite + talc
AK-9	serpentinite	—	—	—	—	serpentinite + chlorite

The symboles mean, ◎ : >20%, ○: <20%, △: <10%, —: not identified.
Abbreviations for minerals, Ol: olivine, Cpx: clinopyroxene, Opx: orthopyroxene, Spl: green spinel.

ture, except the serpentinite (AK-9). Every serpentine exists as a veined structure surrounding olivines and pyroxenes. AK-1 is a dunite composed mostly of olivine with small amounts of clinopyroxene. Very small amounts of serpentine, magnetite, carbonate, and chlorite occur as later stage minerals. AK-2 is also a dunite, which consists entirely of olivine with small amounts of clinopyroxene and green spinel, and little orthopyroxene. Rare amounts of serpentine, magnetite, chlorite, and talc are contained as later stage minerals. AK-3 is a dunite with layered pyroxene-rich bands. The dunite consists of olivine and small amounts of serpentine and magnetite. The pyroxene bands are composed of clinopyroxene and orthopyroxene, with small amounts of opaque minerals, chlorite, and talc. Chromite is very rare. AK-4A is a spinel lherzolite, composed of olivine, orthopyroxene, clinopyroxene, and a small amount of green spinel. Very small amounts of serpentine, magnetite, chlorite, and talc are contained as later stage minerals. This sample is heterogeneous at the microscopic scale. It is composed of pyroxene-rich domains and olivine-rich domains. AK-4B, AK-4C, and AK-5 are similar to AK-4A. AK-6A is a dunite consisting of olivine and small amounts of clinopyroxene, orthopyroxene, and green spinel. Very small amounts of serpentine, magnetite, chlorite, and talc are contained as later stage minerals. AK-6B is a spinel lherzolite consisted of olivine, orthopyroxene, clinopyroxene, and a small amount of green spinel. Some orthopyroxene and green spinel occur as symplectite. Very small amounts of serpentine and magnetite are contained as later stage minerals. AK-7 is a clinopyroxene-rich websterite consisting of clinopyroxene, orthopyroxene and a small amount of green spinel. AK-8 is a dunite consisting of a small amount of opaque minerals and very little green spinel and pyroxene in a lens-shaped area. Very small amounts of serpentine, magnetite, and talc are contained as later stage minerals. AK-9 is a serpentinite with rare chlorite.

Analytical Procedures

The sample rocks were crushed by jaw crusher and stamp mill. After being powdered in an agate mortar, the whole rock sample powders were further finely powdered in an agate ball mill. Clinopyroxene was separated by a magnetic separator and hand picking under a binocular microscope. The concentrations of Rb, Sr, Nd, Sm, Re, and Os were determined by the isotope dilution method.

The analytical method used for the Re-Os isotope systems was as follows. The dissolution of rock powder samples and separation of Re and Os were carried out by the Carius tube method (Shirey and Walker, 1995) and the solvent extraction method (Cohen and Waters, 1996). Fine-grained sample powders (1–3 g) were sealed in a Carius tube with ^{185}Re and ^{190}Os spike solutions and inverse aqua regia and heated at 220°C for 24 hours. After cooling, the solution was moved into a PFA vessel and carbon tetrachloride was added. The vessel with the solution mixture was shaken for 2 min, and the organic solution then filtered from the aqua regia. These processes were repeated three times to complete the Os extraction to the organic phase; Re remained in the acid phase. HBr was then added to the organic fraction and the vessel was again shaken for 2 min. The vessel was kept under a heat lamp for an hour and then chilled in a refrigerator overnight to affect the transfer of Os from the organic fraction to the HBr fraction. The HBr fraction with Os was separated from the organic fraction by filtration. After the HBr was allowed to evaporate until only a small drop remained, and the Os was purified by microdistillation (Roy-Barman, 1993). Rhenium in the acid phase was isolated using anion exchange resin (Bio-rad AG 1X8). The

sample solution of Os and Re were loaded onto a Pt filament. The negative thermal ionization mass spectrometer (N-TIMS) (VG Sector 54-30) at Nagoya University, Japan, was used for Os isotope measurements and Re and Os concentrations with electron multiplier. The average $^{187}Os/^{188}Os$ ratio of the Os standard solution (Osmium plasma standard solution, Specpure, Alfa Aesar) was 0.10643 ± 11 (2σ, $n = 35$). The average of repeated $^{187}Os/^{188}Os$ analyses of the rock reference sample JP-1 was 0.12085 ± 42 (2σ, $n = 5$). Blanks of Re and Os were 0.001 ng, respectively.

The analytical methods used for the Rb-Sr and Sm-Nd isotope systems were as follows. A weighted sample powder was dissolved in $HF\text{-}HClO_4\text{-}HNO_3$, and the elements from the dissolved sample solution were isolated by passing it through cation exchange columns with HCl and 2-methyllactic acid (e.g., Tanaka and Masuda, 1982). Sr and Nd isotope measurements were by TIMS (VG Sector 54-30), and the determinations of Rb, Sr, Sm, and Nd concentrations were made by quadrupole (Q)-TIMS (Finnigan MAT-THQ) at Nagoya University. The average $^{87}Sr/^{86}Sr$ ratio of the NIST-SRM987 standard was 0.710237 ± 17 (2σ, $n = 72$), and the $^{143}Nd/^{144}Nd$ ratio of the JNdi-1 standard solution (Tanaka *et al*., 2000) was 0.512108 ± 10 (2σ, $n = 18$). Blanks of Rb, Sr, Sm, and Nd were 0.5 ng, 2.3 ng, 0.014 ng, and 0.2 ng, respectively. Blanks were negligible in this study. Major elements were analyzed by X-ray fluorescence (XRF) spectroscopy (Sugisaki *et al*., 1977), and minor elements were determined by instrumental neutron activation analysis (INAA, Tanaka *et al*., 1988) at Nagoya University.

RESULTS

The chemical compositions of the Nikubuchi ultramafic rocks are listed in Table 2. MgO content correlates positively with FeO, MnO, Ni, and Co contents, and correlates inversely with SiO_2, Al_2O_3, CaO, TiO_2, Sc, and Cr contents (Fig. 3). The major element contents are related to the modal abundances of the constituent minerals. Sample AK-7, which contains only clinopyroxene, orthopyroxene and no olivine, has the lowest MgO content. Most minerals in sample AK-9 had been altered to serpentine. The plot for sample AK-9 lies slightly apart from the correlation line drawn through the data points of the other samples that contain little serpentine (Fig. 3).

The Rb, Sr, Nd, and Sm concentrations and Sr and Nd isotope ratios are shown in Table 3. The Rb concentrations vary from 0.021 to 0.44 ppm. The Sr concentrations of whole rock samples (2.6–68 ppm) correlate well with the Rb concentrations, while the Rb and Sr concentrations are inversely correlated with the concentration of MgO ($r = -0.95$ for both elements). The Rb and Sr corre-

Table 2. The abundances of major and trace elements in the Nikubuchi ultramafic rocks

		SiO_2	TiO_2	Al_2O_3	FeO*	MnO	MgO	CaO	Na_2O	K_2O	P_2O_5	LOI	Total	Sc	Cr	Co	Ni	Zn	Mg#
AK-1	dunite	37.3	0.01	0.24	16.4	0.27	39.3	0.27	n.d.	n.d.	0.006	4.46	98.2	5.5	149	180	630	76	0.81
AK-2	dunite	37.4	0.02	1.42	15.6	0.24	38.0	1.03	n.d.	n.d.	0.006	4.52	98.2	7.6	649	182	578	73	0.81
AK-3	dunite	38.1	0.02	0.38	15.7	0.26	40.3	0.83	n.d.	n.d.	0.005	3.00	98.6	7.9	206	190	588	81	0.82
AK-4A	spinel lherzolite	41.5	0.12	1.98	12.8	0.20	33.8	6.32	0.02	n.d.	0.007	1.47	98.3	29.9	958	143	458	71	0.82
AK-4B	spinel lherzolite	40.8	0.07	1.33	13.9	0.23	37.0	4.23	n.d.	n.d.	0.006	1.98	99.5	21.4	621	161	636	83	0.83
AK-4C	spinel lherzolite	45.7	0.26	4.74	7.9	0.13	21.2	15.43	0.18	n.d.	0.006	1.02	96.5	68.1	2261	77	243	118	0.83
AK-5	spinel lherzolite	43.4	0.16	3.75	10.9	0.17	26.8	10.52	0.09	0.003	0.006	1.96	97.8	46.4	2025	114	480	94	0.81
AK-6A	dunite	37.0	0.02	0.21	15.8	0.25	38.9	0.52	n.d.	n.d.	0.005	4.35	97.1	5.9	151	174	707	68	0.81
AK-6B	spinel lherzolite	42.5	0.12	2.18	12.4	0.19	32.1	7.60	0.07	n.d.	0.005	2.58	99.8	32.8	1546	128	578	80	0.82
AK- 7	websterite	47.1	0.28	6.63	7.3	0.11	17.8	17.23	0.35	0.004	0.005	0.50	97.4	68.5	3658	62	316	73	0.81
AK-8	dunite	37.4	0.02	0.28	15.0	0.25	39.4	0.70	n.d.	n.d.	0.005	5.56	98.6	6.5	122	173	905	76	0.82
AK-9	serpentinite	37.6	0.05	2.07	14.9	0.19	33.1	0.51	n.d.	n.d.	0.005	10.45	98.8	13.1	182	129	432	68	0.80

Major element concentrations are in wt%, and trace elements abundances are in ppm. The n.d. means below detection limit.
FeO: total iron expressed as FeO. LOI: loss on ignition measured by the gravimetric method. Mg#: Mg/(Mg + total Fe) atomic ratio in whole rock.*

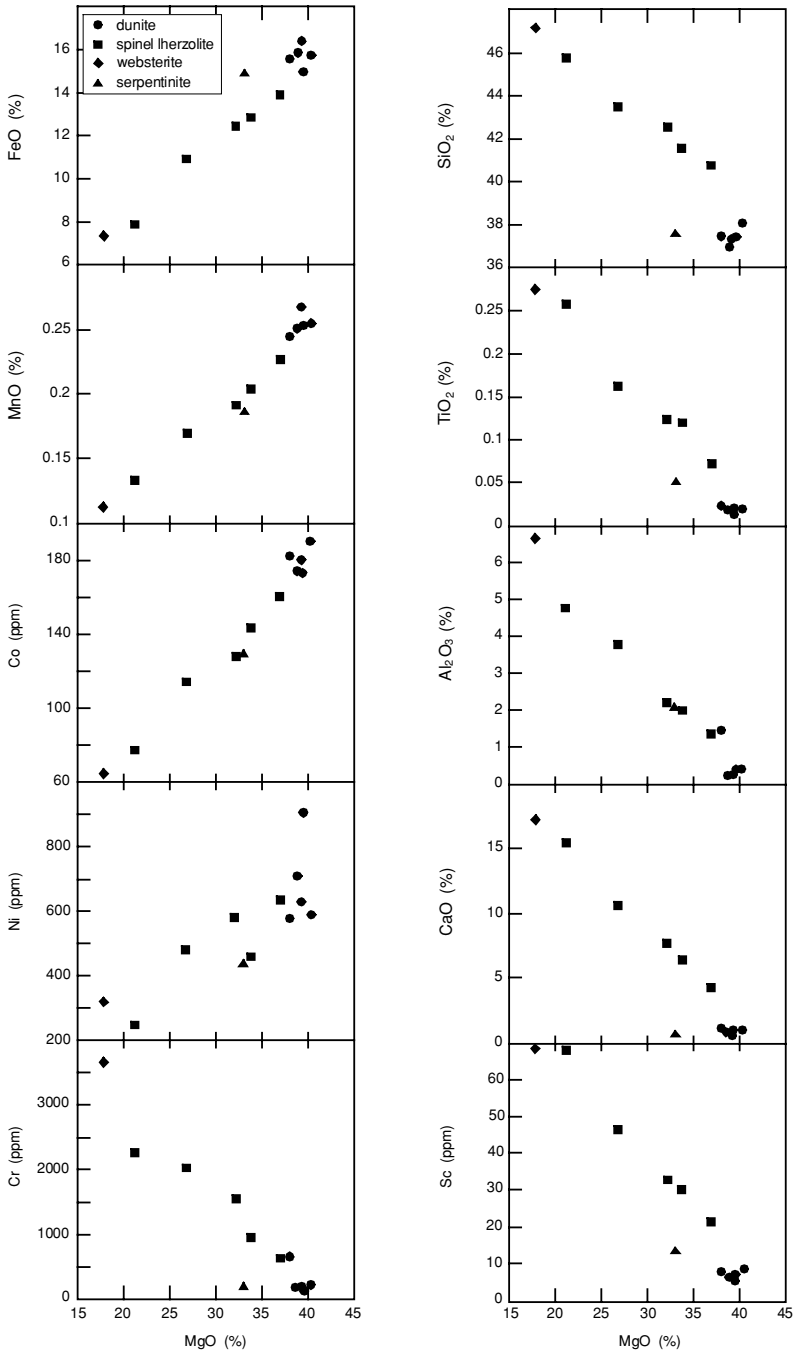

Fig. 3. MgO diagrams for Al_2O_3, CaO, FeO, MnO, SiO_2, TiO_2, Co, Cr, Ni, and Sc for the Nikubuchi ultramafic rocks.

lations with other major elements are also high ($r = \pm 0.9$). The Rb and Sr abundances are enriched in spinel lherzolite and low in dunite. Because of the very low abundance and small variation of Rb, the accumulation of radiogenic ^{87}Sr over geological time was very small, and the Sr isotope ratios are similar to each other, ranging from 0.7044 to 0.7049. The Nd and Sm concentrations (Nd, 0.032–2.8 ppm; Sm, 0.01–1.3 ppm) also vary widely and correlate well with each other ($r = 0.9998$), but they do not clearly correlate with MgO abundance. The abundances of Nd and Sm are lower in dunites than in the other rocks. The Nd isotope ratios show more variation in dunites ($^{143}Nd/^{144}Nd = 0.51281–0.51294$) than in spinel lherzolite ($^{143}Nd/^{144}Nd = 0.51293–0.51296$). The Nd isotope ratio of the clinopyroxene is higher than that of whole rock in AK-3 (dunite). On the other hand, the Nd isotope ratios of

Table 3. Sr and Nd isotopic compositions and Rb, Sr, Nd, and Sm concentrations in the Nikubuchi ultramafic rocks

		Rb	Sr	$^{87}Rb/^{86}Sr$	$^{87}Sr/^{86}Sr$	Nd	Sm	$^{147}Sm/^{144}Nd$	$^{143}Nd/^{144}Nd$	$\varepsilon_{Nd138Ma}$*
AK-1	dunite	0.044	4.5	0.027 ± 1	0.70487 ± 2	0.032	0.010	0.187 ± 13	0.512814 ± 85	3.6
AK-2	dunite	0.033	8.0	0.012 ± 1	0.70451 ± 2	0.057	0.017	0.179 ± 8	0.512852 ± 8	4.5
AK-3	dunite	0.046	5.5	0.024 ± 1	0.70460 ± 2	0.066	0.026	0.240 ± 1	0.512935 ± 19	5.0
AK-3-c	cpx		34.9		0.71384 ± 3	1.828	0.820	0.271 ± 1	0.512980 ± 41	5.4
AK-4A	spinel lherzolite	0.067	13.7	0.014 ± 1	0.70441 ± 1	0.451	0.210	0.282 ± 2	0.512956 ± 8	4.7
AK-4B	spinel lherzolite	0.068	9.0	0.021 ± 1	0.70447 ± 2	0.278	0.129	0.281 ± 3	0.512948 ± 8	4.6
AK-4C	spinel lherzolite	0.439	36.6	0.034 ± 1	0.70468 ± 1	1.430	0.647	0.273 ± 1	0.512951 ± 10	4.8
AK-4C-c	cpx		36.5		0.71035 ± 3	1.966	0.870	0.267 ± 1	0.512946 ± 9	4.8
AK-4C-r	residue		24.6		0.70440 ± 2	0.954	0.431	0.273 ± 1	0.512976 ± 73	5.3
AK-5	spinel lherzolite	0.263	35.2	0.021 ± 1	0.70451 ± 2	0.771	0.337	0.264 ± 1	0.512931 ± 8	4.5
AK-6A	dunite	0.047	2.6	0.052 ± 5	0.70447 ± 2	0.073	0.014	0.115 ± 1	0.512830 ± 52	5.2
AK-6B	spinel lherzolite	0.108	12.1	0.025 ± 1	0.70451 ± 2	0.510	0.223	0.265 ± 2	0.512941 ± 8	4.7
AK-7	websterite	0.355	67.9	0.015 ± 1	0.70451 ± 2	1.373	0.614	0.270 ± 2	0.512943 ± 9	4.7
AK-7-c	cpx		80.2		0.70506 ± 3	1.808	0.797	0.267 ± 1	0.512956 ± 11	5.0
AK-7-r	residue		43.6		0.70679 ± 3	0.878	0.396	0.272 ± 1	0.512962 ± 21	5.0
AK-8	dunite	0.021	4.4	0.013 ± 1	0.70464 ± 1	0.042	0.012	0.168 ± 5	0.512855 ± 5	4.7
AK-9	serpentinite	0.072	10.7	0.019 ± 1	0.70470 ± 2	0.143	0.042	0.179 ± 1	0.512800 ± 8	3.5

The abundances of Rb, Sr, Nd and Sm are in ppm. All errors are 2σ.
$\varepsilon_{Nd138Ma} = [((^{143}Nd/^{144}Nd)_{Sample}/(^{143}Nd/^{144}Nd)_{CHUR(138Ma)}) - 1] \times 10^4$, $(^{143}Nd/^{144}Nd)_{CHUR(0)} = 0.512638$, $(^{147}Sm/^{144}Nd)_{CHUR} = 0.1967$ (Wasserburg et al., 1981).

Table 4. Re and Os concentrations, and Os isotope ratios in the Nikubuchi ultramafic rocks

	Re (ppb)	Os (ppb)	$^{187}Os/^{188}Os$[a]	$^{187}Re/^{188}Os$[a]	$^{187}Os/^{188}Os_{(138Ma)}$[b]
AK-1	0.29	0.079	0.1536 ± 61	17.3 ± 0.7	0.114
AK-2	1.10	0.165	0.1687 ± 12	31.5 ± 4.8	0.096
AK-3	0.12	0.112	0.1727 ± 72	4.9 ± 0.7	0.161
AK-4A	0.37	0.092	0.2052 ± 20	18.8 ± 2.9	0.162
AK-4B	1.77	0.162	0.1890 ± 21	51.5 ± 6.6	0.071
AK-4C	2.66	0.565	0.2063 ± 85	22.2 ± 12.5	0.155
AK-5	0.54	0.075	0.2651 ± 294	33.8 ± 7.8	0.188
AK-6A	0.11	0.128	0.1657 ± 15	3.9 ± 0.4	0.157
AK-6B	0.72	0.129	0.2526 ± 210	26.3 ± 5.4	0.192
AK-7	1.63	0.128	0.2436 ± 62	60.4 ± 1.8	0.105
AK-8	1.64	0.107	0.1962 ± 16	72.6 ± 0.7	0.030
AK-9	0.38	0.041	0.2382 ± 17	43.0 ± 1.5	0.140

a: The errors of $^{187}Os/^{188}Os$ and $^{187}Re/^{188}Os$ are 2σ.
b: The $^{187}Os/^{188}Os_{(138Ma)}$ values are calculated from the age of Nd isochron 138Ma and used: $\lambda^{187}Re = 1.666 \times 10^{-11}$ yr^{-1} (Smoliar et al., 1996).

clinopyroxene and residues from spinel lherzolite and websterite correspond to those of whole rocks within these errors.

The Re and Os concentrations and Os isotope compositions are shown in Table 4. The Re concentrations range from 0.11 to 2.66 ppb. The Os concentrations range from 0.041 to 0.565 ppb. Re and Os concentrations are not correlated with each other, and neither correlates well with major elements or the other minor elements. The $^{187}Re/^{188}Os$ ratios range between 3.9 and 72.6, while Os isotope ratios range between 0.154 and 0.265. The dunites generally show lower $^{187}Os/^{188}Os$ ratios than the spinel lherzolites. It is expected that the Re-Os isotope system relates to the modal composition of the minerals (Fig. 4). The Re and Os concentrations of sample AK-4C are higher than those of the other samples, but the Os isotope ratio and the Re/Os ratio of the sample are similar to those of other samples (Table 4). The low Os abundance and the Re enrichment in samples AK-4B, AK-7, and AK-8 result in high Re/Os ratios in those samples (Table 4). The

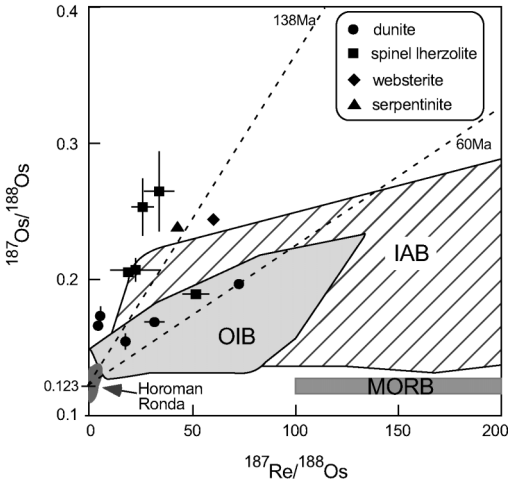

Fig. 4. $^{187}Os/^{188}Os$ vs. $^{187}Re/^{188}Os$ of the ultramafic rocks in the Nikubuchi complex with ultramafic rocks from the Horoman and Ronda complexes derived from the upper mantle, IAB, MORB, and OIB. The error bars show 2σ. The dot lines mean the reference isochrons of 138 Ma and 60 Ma with initial isotope ratio of depleted MORB mantle ($^{187}Os/^{188}Os$ = 0.123). The data for the Horoman and Ronda complexes are from Liu and Tanaka (1999), Saal et al. (2001), and Reisberg et al. (1991). The data of IAB, MORB and OIB are from Alves et al. (2002), Hauri and Hart (1993), Hauri and Kurz (1997), Reisberg et al. (1993), and Shirey and Walker (1998).

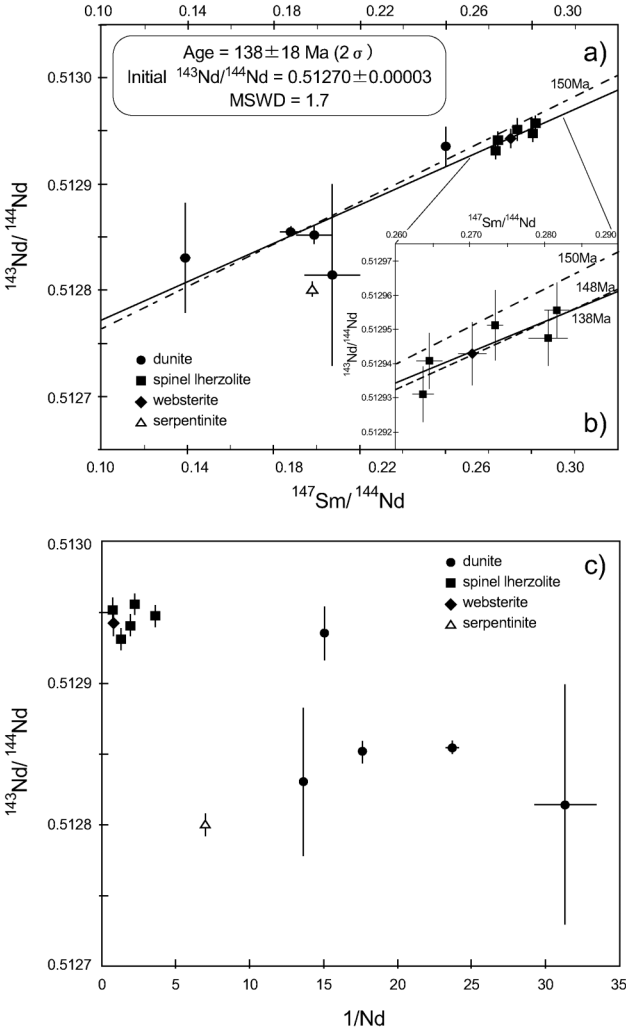

Fig. 5. a) $^{143}Nd/^{144}Nd$ vs. $^{147}Sm/^{144}Nd$ of the Nikubuchi ultramafic rocks. The data form an isochron of 138 Ma, except for serpentinite AK-9 (open triangle). The error bars show 2σ. The dashed and single-dotted line means an isochron of 150 Ma from the dunites. Age computation was performed using the ISOPLOT program (Ludwig, 2001). b) $^{143}Nd/^{144}Nd$ vs. $^{147}Sm/^{144}Nd$ among the spinel lherzolite and websterite show an isochron of 148 Ma (dashed line). The initial ratios of the isochrons are shown in the text. c) $^{143}Nd/^{144}Nd$ vs. 1/Nd values for the Nikubuchi ultramafic rocks. These plots could not verify mixing.

Os isotope ratios of the samples from the Nikubuchi complex are similar to those of both the Horoman complex, which is another ultramafic layered massif in the Japanese islands (0.116–0.128; Liu and Tanaka, 1999; Saal *et al*., 2001), and the Ronda ultramafic complex in southern Spain (0.117–0.132; Reisberg *et al*., 1991). However, the Os concentrations of the samples from the Nikubuchi complex are lower than those from Horoman (2.34–56 ppb; Liu and Tanaka, 1999; Saal *et al*., 2001) and Ronda (2.5–6.7 ppb; Reisberg *et al*., 1991). The Re/Os ratios of the Nikubuchi rocks ($^{187}Re/^{188}Os$ = 3.9–72.6) are higher than those of the Horoman complex ($^{187}Re/^{188}Os$ = 0.007–0.585; Saal *et al*., 2001) and Ronda complex ($^{187}Re/^{188}Os$ = 0.02–0.63; Reisberg *et al*., 1991) as well.

Discussion

Sm-Nd whole-rock isochron age

We obtained a correlation line for the Sm-Nd isotope system. If the line is an isochron, it indicates an age of 138 ± 18 (2σ) Ma with an initial $^{143}Nd/^{144}Nd$ ratio of 0.51270 ± 3 (except sample AK-9, which has been altered to serpentinite) (Fig. 5a). Before discussing what event this age indicates, we will confirm that this line is an isochron by reviewing two requirements that must be met: 1) the whole Nikubuchi complex had equilibrated isotopically, 2) the line was not formed by mixing.

The lithologic study revealed that the Nikubuchi complex was made up of igneous rocks composed of the continuous cumulous minerals in a magma chamber, and did not derive from lava flow and plural intrusive rock (Yokoyama, 1980). The major and trace element abundances vary consistently with MgO abundance (Fig. 3). This indicates that the complex formed through fractional crystallization from a single magma chamber. To confirm

the isotopic equilibrium on the whole Nikubuchi complex, regardless of the lithology, isochrons were drawn on the dunites only and on the spinel lherzolites and websterite, respectively. The isochron of the dunites, which have relatively low Sm/Nd ratios, indicates an age of 150 ± 130 Ma with $^{143}Nd/^{144}Nd_{(i)}$ = 0.51269 ± 16 (Fig. 5a). The isochron among the spinel lherzolites and websterite indicates an age of 148 ± 74 Ma with $^{143}Nd/^{144}Nd_{(i)}$ = 0.51268 ± 13 (Fig. 5b). These ages have relatively large errors because the variation of the Sm/Nd ratios is small in this restricted rock type. Though there is significant uncertainty regarding these ages, these results are similar to the age of the whole Nikubuchi complex. The initial Nd isotope ratios of these two isochrons agree with the initial Nd isotope ratio from the whole Nikubuchi complex within an acceptable error. The agreement of these initial Nd isotope ratios indicates that the dunites and spinel lherzolites of the Nikubuchi complex have experienced isotopic equilibrium.

Evidence that the correlation line does not represent a mixing line includes the following: First, no apparent correlation between the $^{143}Nd/^{144}Nd$ ratios and 1/Nd values is observed (Fig. 5c). Second, the Nd isotope ratios and Sm/Nd ratios of dunites and spinel lherzolites vary in accordance with the rock type, and independently of the sampling position (Fig. 5a). Third, trace element abundances show consistent variation with MgO abundance (Fig. 3). If the Nikubuchi complex was formed by the mixing of two or more different sources, element abundance would show several different variation trends and the relationship would not be linear (i.e., the differentiation curve would not be straight). Consequently, the line is regarded as an isochron, indicating an age of 138 ± 18 (2σ) Ma and an initial $^{143}Nd/^{144}Nd$ ratio of 0.51270 ± 3 (Fig. 5a).

The Nd isotope ratios and Sm/Nd ratios of the separated mineral samples are similar to those of the whole rock samples for both spinel lherzolite and websterite. The separated clinopyroxene and residual phase values are similar, in part because the residues still contain a significant amount of clinopyroxene. Complete mineral separation was impossible because the veined complex structures were present in mineral grains, and because clinopyroxene and orthopyroxene sometimes form symplectites.

The meaning of the Sm-Nd whole-rock isochron age and origin of the Nikubuchi ultramafic complex

The isochron age shows either the age of the magmatic formation, granulite facies metamorphism, serpentinization, epidote-amphibolite facies metamorphism (the Sambagawa metamorphism) (Yokoyama, 1980; Kunugiza, 1984), or hydration metamorphism occurring on the surrounding Iratsu epidote amphibolite mass during uplifting (Takasu, 1989). Serpentinization and hydration during uplifting result in the addition of elements to the complex from outside and/or extraction of elements from the complex. It is important to know the elements' host phase when considering the influence of metamorphism and movement of the elements. Lithophile element concentrations are higher in spinel lherzolites than in dunite, suggesting that the lithophile elements are mainly distributed in pyroxene. In fact, the Sr, Nd, and Sm concentrations in clinopyroxenes are higher than those in whole rocks (Table 3). According to the element partition coefficients between mineral and melt in the ultramafic rocks (Shaw, 2000), the partition coefficients of Nd and Sm in clinopyroxene (Nd: 0.1873, Sm: 0.291, Sm/Nd = 1.6) are larger than those in olivine (Nd: 0.000398, Sm: 0.00065, Sm/Nd = 1.6), orthopyroxene (Nd: 0.00052, Sm: 0.0016, Sm/Nd = 3.1), and spinel (Nd: 0.0002, Sm: 0.0004, Sm/Nd = 2.0). This suggests that Nd and Sm are mainly contained in clinopyroxene and are largely absent from olivine and orthopyroxene. Even in dunite (AK-3), Sr, Nd, and Sm are contained predominantly in clinopyroxene. The samples of dunites also contain 10 wt% or smaller amounts of clinopyroxene (Table 1). Serpentinization and the hydration effect are strong for both olivine and orthopyroxene, and relatively weak for clinopyroxene, but it is unlikely that isotopic equilibrium has been reached across the entire Nikubuchi complex solely as a consequence of these events. Other events that may have reset the isotope systems are magmatic formation, granulite facies metamorphism, and epidote-amphibolite metamorphism.

The previous petrological study of the Nikubuchi complex enables the Sm-Nd whole rock isochron age to be distinguished from the age of the Sambagawa metamorphism. Three main factors could serve to exclude the possibility that the Sambagawa metamorphism is responsible for the isochron age: 1) each sample retains the protogranular texture, 2) the major and trace element abundances plot on single lines with MgO abundance (Fig. 3), and 3) several reports show that clinopyroxene sometimes holds older isotopic information than garnet (Mørk and Mearns, 1986; El-Naby *et al*., 2000). The Sm-Nd system in this study is strongly dependant on the modal abundance of clinopyroxene.

We now consider each of these factors in detail. According to Yokoyama (1980), all the rock types of the Nikubuchi complex have protogranular texture. Mineral assemblages underwent limited reconstruction as a consequence of the Sambagawa metamorphism, and almost all of the previous mineral assemblage remained unchanged. Because the proto granular mineral texture was retained during the Sambagawa metamorphism, it is hard to assume isotopic equilibrium completely in the whole

Nikubuchi complex. The pyroxene re-equilibrium texture surrounded by hornblende and garnet during the Sambagawa metamorphism was reported by Yokoyama (1980). This texture, however, is not observed in the thin sections of this study.

Regarding factor 2): if elements migrated during the metamorphism, element abundances would be plotted as multiple trends, which reflect the lithology, as has been observed in studies of other ultramafic massifs (Takazawa *et al*., 1999; Chalot-Prat *et al*., 2003; Niu, 2004), rather than as a single line, as observed here in the Nikubuchi complex. In fact, the SiO_2 and TiO_2 abundances in the serpentinite affected by hydration, and dunites which have relatively large LOI values (Table 2), are plotted slightly out of synchronization on the spinel lherzolite line to demonstrate this (Fig. 3).

Regarding factor 3), the Sm/Nd ratios in Nikubuchi complex sample agree well with CaO abundances, which are the main component of clinopyroxene. Thin section observation indicates that the minerals olivine, clinopyroxene, and orthopyroxene are dominant in all the samples. There are no host minerals of rare earth elements such as garnet, apatite, hornblende, or phlogopite. This suggests that the Sm-Nd system of the whole Nikubuchi complex depends on the clinopyroxene. In general, clinopyroxene and garnet were used for the isotopic analysis of Rb-Sr and Sm-Nd in the ultramafic xenoliths and metagabbro. The closure temperature of the Sm-Nd system in garnet is 700–750°C (Möller *et al*., 2002). Mørk and Mearns (1986) and El-Naby *et al*. (2000) reported that clinopyroxene sometimes retains older isotopic information than does garnet. The closure temperature of clinopyroxene would be comparable to or higher than that of garnet. The temperature of the Sambagawa metamorphism (600°C) is lower than the closure temperature of the garnet, and consequently the isotopic re-equilibrium of the Sm-Nd system in the whole Nikubuchi complex during the Sambagawa metamorphism is unlikely.

Okamoto *et al*. (2004) reported the U-Pb ages of metamorphic zircon rims (112–132 Ma) from the quartz-bearing eclogite, and these ages are consistent with the peak age of the Sambagawa metamorphism (100–120 Ma). They also reported the zircon core ages (134–148 Ma), which provide a maximum deposition age for the sandstones of the SMB. Isozaki and Itaya (1990) compiled fossil ages of the protoliths and radiogenic ages of the SMB and concluded that sediment deposition occurred at about 130 Ma. For the reasons stated above, it is reasonable to suppose that the Sm-Nd whole-rock isochron age of 138 Ma indicates the event which occurred before the Sambagawa metamorphism. The event that occurred at 138 Ma is believed to be either the magmatic formation or the granulite facies metamorphism. It is difficult, however, to confirm this as the age of the formation or the granulite facies metamorphism.

Enami (2002) re-examined the equilibrium temperature of the coexistent granulite and estimated the P-T path of the samples from the Nikubuchi complex. He pointed out the possibility that the Nikubuchi complex formed under granulite facies P-T conditions before being affected by the Sambagawa metamorphism. If that were the case, the Nikubuchi complex would not necessarily have been affected by the granulite facies metamorphism after formation. The Nikubuchi complex formed as an igneous cumulous complex in a magma chamber at granulite facies, and the rocks in the complex have a granular texture. Under this scenario, the Sm-Nd whole-rock isochron age equals the formation age of the Nikubuchi complex. The initial ε_{Nd} values at 138 Ma of the Nikubuchi complex (ε_{Nd} = +3.5 to +5.3) correspond to values for both ocean island basalt (OIB, ε_{Nd} = –2 to +10), and island arc basalt (IAB, ε_{Nd} = –4 to +10), but are not in the range of mid-ocean ridge basalt (MORB) values (ε_{Nd} = +6 to +13). The Nd isotope ratios alone do not allow the origin of the Nikubuchi complex to be determined as being either OIB or IAB. The Iratsu epidote-amphibolite mass that surrounds the Nikubuchi complex is included in the sedimentary rocks of the accretionary prism. From the lithologic study, the protolith of the Iratsu epidote-amphibolite mass was layered gabbro (Banno *et al*., 1976) and had been taken into the surrounding sedimentary rocks before the Sambagawa metamorphism (Takasu and Kohsaka, 1987; Toriumi and Kohsaka, 1995). The Nikubuchi complex is also included in the accretionary prism's sedimentary rocks. Therefore, the OIB magma, which erupted on the subducting oceanic plate, is presumed to be the original magma of the Nikubuchi complex, rather than the IAB, which erupted on the mantle wedge side at the subduction zone.

Sr and Os isotope ratios

The Rb-Sr isotope system has no significant isochron trend at present (Fig. 6). The calculated Sr isotope ratio at 138 Ma differs little from the measured (at present) Sr isotope ratios because of very low Rb concentrations. The Rb contribution to ^{87}Sr for each sample is less than 1×10^{-4} of the $^{87}Sr/^{86}Sr$ ratio over 138 million years. The dunites have higher Sr isotope ratios than the spinel lherzolites. This disagreement shows that, in contrast to the Sm-Nd system, a disturbance of the Rb-Sr system occurred. This disturbance cannot be explained by simple models, however, such as contamination and extraction by hydration or metamorphism. Rb-Sr systems are more easily disturbed than Sm-Nd systems, so the disturbance of the Rb-Sr system reflects an event younger than 138 Ma.

The Re-Os system of the Nikubuchi complex also has no clear isochron trend (Fig. 4). In Fig. 4, the samples

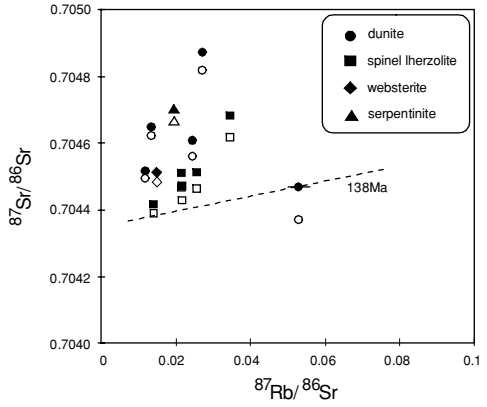

Fig. 6. $^{87}Sr/^{86}Sr$ vs. $^{87}Rb/^{86}Sr$ in the Nikubuchi ultramafic rocks. The solid symbols indicate the present values and the open symbols are calculated values for 138 Ma. The error bars show 2σ. The dot line means 138 Ma slope.

with high $^{187}Re/^{188}Os$ ratios do not always have high $^{187}Os/^{188}Os$ ratios, and the $^{187}Os/^{188}Os$ ratios of low $^{187}Re/^{188}Os$ ratio samples is in some cases higher than the $^{187}Os/^{188}Os$ ratio of high $^{187}Re/^{188}Os$ ratio samples (Table 4). These disagreements suggest that the Rb-Sr and Re-Os systems were disturbed by hydration after 138 Ma, or might not have been completely reset in whole rocks of the Nikubuchi complex by the granulite facies or the Sambagawa metamorphisms.

Re-enrichment

Calculation of the Os isotope ratio at 138 Ma indicates that some samples have an isotope ratio lower than MORB at 138 Ma (Table 4). This indicates that the Re-Os isotope system of the Nikubuchi complex has been disturbed at an age younger than 138 Ma. Because the $^{187}Re/^{188}Os$ ratios in other ultramafic complexes are low (Fig. 4), the Re-Os system in the Nikubuchi complex seems to have experienced Re enrichment rather than the addition of Os from the surroundings. The Os isotope ratios became high compared with the other ultramafic complexes (Fig. 4) through the decay of ^{187}Re. Chesley *et al.* (2004) showed that Re is more mobile than Os during subduction zone metasomatism, with Re easily extracted into fluid compared with Os (Burnham *et al.*, 1998; Righter *et al.*, 1998). Study of a dunite vein in the Troodos Ophiolite Complex shows that Re is more enriched in the vein than in the surrounding harzburgite (Büchl *et al.*, 2002). It is possible that the Re in the ultramafic rocks from the Nikubuchi complex was also influenced by fluid. The Iratsu epidote-amphibolite mass surrounding the Nikubuchi complex was affected by strong hydration during uplifting; the eclogite was hydrated and formed amphibolite (Takasu, 1989). It is possible that the same hydration has affected the Nikubuchi complex and caused the addition of Re.

When considering the timing of this hydration event, we assumed that the origin of the Nikubuchi complex was the cumulate from magma extracted from the depleted mantle (MORB). MORB has lower Os isotope ratios than OIB and IAB. The isotope ratios of MORB are generally homogeneous. Magmatic solidification is assumed to have occurred quickly after the magma was extracted from the mantle. We calculated the age that would be needed for the Re-Os system values in the Nikubuchi complex to reach the Os isotope ratio of MORB (0.123). It is expected that this calculated result represents the oldest estimation of Re contamination. The youngest calculated age (60 Ma) among the samples of the Nikubuchi complex was obtained from the AK-8 (dunite), which has the highest Re/Os ratio (Table 4). If the hydration age is older than 60 Ma, then the initial Os ratio of AK-8 is calculated to be lower than that of MORB, which has the lowest value of any terrestrial material. The dunite, which is composed primarily of olivine, is more easily affected by hydration than the spinel lherzolite, which is composed of olivine, clinopyroxene, and orthopyroxene. Although the dunite samples have low Os isotope ratios, most of the dunites have a high Re/Os ratio (Fig. 4). The addition of Re to the AK-8 layer must have occurred at or subsequent to 60 Ma. Moreover, the Nd initial value suggests that the Nikubuchi complex originated from the magma cumulate, which had higher Os isotope ratios (i.e., had values characteristic of OIB and IAB, rather than the depleted ratio of MORB). If this is the case, then the assumed initial Os isotope ratio is higher than that calculated above, and the slope between the assumed initial Os isotope ratio and AK-8 in Fig. 4 becomes moderately lower. The ages obtained for the origin of OIB and IAB are younger than 60 Ma. It is difficult to estimate the valid initial Os isotope ratio of the whole Nikubuchi complex because of the later disturbance, to differing degrees, in the Re-Os systems. The oldest age of the Re addition is 60 Ma, however, which clearly distinguishes it from the Sm-Nd whole-rock isochron age. This strongly supports the conclusion that hydration could not affect the Sm-Nd system inside minerals.

The Besshi nappe complex, including the Nikubuchi complex, underwent the Sambagawa metamorphism at 100–120 Ma and was then uplifted to the surface. Takasu and Dallmeyer (1990) measured the $^{40}Ar/^{39}Ar$ age of the hornblendes and muscovites from the entire Besshi area. Their results indicate that the hornblendes, which have a closure temperature of about 500°C, show an age of 78–87 Ma; the muscovites have a closure temperature 350–400°C, with an age of 76–86 Ma. These ages indicate the cooling history of the Besshi area. The timing of the post-60 Ma hydration, presumed from the Re-Os isotope sys-

tem evidence, occurred after the stage cooled below 350°C. Therefore, the hydration occurred during the uplifting of the Besshi area, after the Sambagawa metamorphism. At that time, the pressure condition of the whole Besshi nappe was below 0.5 GPa (Takasu, 1989). This pressure corresponds to a depth of less than 20 km, and indicates that hydration occurred in a shallow situation.

Conclusions

The chemical and Os, Nd, and Sr isotopic compositions of the Nikubuchi ultramafic complex, which has a structure of igneous cumulate, were analyzed. An age of 138 ± 18 Ma, with an initial $^{143}Nd/^{144}Nd$ ratio of 0.51270 ± 3, was acquired from the Sm-Nd whole-rock isochron. This age indicates either the age of the magmatic formation or the synchronous granulite facies metamorphism before the Sambagawa metamorphism. The latter was excluded as a possibility in part because the Nikubuchi complex samples have retained the mineral assemblage of the granulite. The $\varepsilon_{Nd(138Ma)}$ values are identical to the $\varepsilon_{Nd(138Ma)}$ value of OIB and IAB, rather than that of MORB. Because the Nikubuchi complex is incorporated into the accretionary prism sediments at present, the origin of the Nikubuchi complex is likely the cumulate that consists of the residue of OIB magma. The Rb-Sr isotope systems were disturbed by metamorphism and/or hydration after 138 Ma. The Re-Os isotope system also failed to show a valid isochron. One possible explanation is that Re addition occurred after 138 Ma, and probably subsequent to 60 Ma. This corresponds to the fact that the Iratsu epidote-amphibolite mass surrounding the Nikubuchi complex has been affected by hydration during uplifting. According to the previous studies of the SMB, the Besshi nappe, including the Nikubuchi complex, settled at a depth equal to or less than 20 km from the surface, subsequent to 60 Ma. Hydration occurred at a shallow region and not at a deeper location near the subduction zone. The data from this study show that hydration disturbed the Re-Os system but did not affect the Sm-Nd system. This result appears to reflect differences in the host phase of each element. It is thought that Re and Os exist mainly in the olivine and/or intergranular minerals, and are easily affected by metamorphism and hydration. In contrast, Sm and Nd are distributed inside the pyroxene, which is resistant to these events. As the maximum age of the hydration could be declared by the Re-Os system of this study, there is a possibility for the Re-Os system to estimate the age and effect of the metamorphism or hydration.

Acknowledgments—We thank Professors Masaki Enami and Takashi Agata for their helpful petrological suggestions. We also thank Dr. Kazumi Yokoyama for teaching us about the geology of the sampling area. Grateful thanks go to Dr. Tomoyuki Shibata and the anonymous reviewers for careful reviews and helpful suggestions. Drs. Masayo Minami and Yoshihiro Asahara kindly helped us with the mass spectrometry. Special thanks are also due to Mr. Shigeo Yoshioka and Mr. Setsuo Yogo for their help in preparing glass instruments and thin sections. A part of the work was supported by the 21st Century COE Program G-4 "Dynamics of the Sun-Earth-Life Interactive System" the Ministry of Education, Culture, Sports, Science and Technology.

References

Alves, S., Schiano, P., Capmas, F. and Allègre, C. J. (2002) Osmium isotope binary mixing arrays in arc volcanism. *Earth Planet. Sci. Lett.* **198**, 355–369.

Banno, S., Yokoyama, K., Iwata, O. and Terashima, S. (1976) Genesis of epidote amphibolite masses in the Sanbagawa metamorphic belt of central Shikoku. *J. Geol. Soc. Jpn.* **82**, 199–210 (in Japanese with English abstract).

Büchl, A., Brügmann, G., Batanova, G., Münker, C. and Hofmann, A. W. (2002) Melt percolation monitored by Os isotopes and HSE abundances: a case study from the mantle section of the Troodos Ophiolite. *Earth Planet. Sci. Lett.* **204**, 385–402.

Burnham, O. M., Rogers, N. W., Pearson, D. G., van Calsteren, P. W. and Hawkesworth, C. J. (1998) The petrogenesis of the eastern Pyrenean peridotites: An integrated study of their whole-rock geochemistry and Re-Os isotope composition. *Geochim. Cosmochim. Acta* **62**, 2293–2310.

Chalot-Prat, F., Ganne, J. and Lombard, A. (2003) No significant element transfer from the oceanic plate to the mantle wedge during subduction and exhumation of the Tethys lithosphere (Western Alps). *Lithos* **69**, 69–103.

Chesley, J., Righter, K. and Ruiz, J. (2004) Large-scale mantle metasomatism: a Re-Os perspective. *Earth Planet. Sci. Lett.* **219**, 49–60.

Cohen, A. S. and Waters, F. G. (1996) Separation of osmium from geological materials by solvent extraction for analysis by thermal ionization mass spectrometry. *Anal. Chim. Acta* **332**, 269–275.

El-Naby, H., Frisch, W. and Hegner, E. (2000) Evolution of the Pan-African Wadi Haimur metamorphic sole, Eastern Desert, Egypt. *J. Metamorph. Geol.* **18**, 639–651.

Enami, M. (1982) Oligoclase-biotite zone of the Sanbagawa metamorphic terrane in the Bessi district, central Shikoku, Japan. *J. Geol. Soc. Jpn.* **88**, 887–900 (in Japanese with English abstract).

Enami, M. (2002) Re-estimation of equilibrium conditions of granilitic assemblages in the Nikubuchi mass of the Sanbagawa belt, central Shikoku, Japan. *Abstract for 109th Annual Meeting of the Geological Society of Japan*, p. 167 (in Japanese).

Hauri, E. H. and Hart, S. R. (1993) Re-Os isotope systematics of HIMU and EM2 oceanic island basalts from the South Pacific Ocean. *Earth Planet. Sci. Lett.* **114**, 353–371.

Hauri, E. H. and Kurz, M. D. (1997) Melt migration and mantle chromatography, 2: a time-series Os isotope study of Mauna Loa volcano, Hawaii. *Earth Planet. Sci. Lett.* **153**, 21–36.

Higashino, T. (1975) Biotite zone of Sanbagawa metamorphic terrain in the Shiragayama area, central Shikoku, Japan. *J. Geol. Soc. Jpn.* **81**, 653–670 (in Japanese with English abstract).

Isozaki, Y. and Itaya, T. (1990) Chronology of Sanbagawa metamorphism. *J. Metamorph. Geol.* **8**, 401–411.

Itaya, T. and Takasugi, H. (1988) Muscovite K-Ar ages of the Sanbagawa schists, Japan, and argon depletion during cooling and deformation. *Contrib. Mineral. Petrol.* **100**, 281–290.

Kojima, G., Hide, K. and Yoshino, G. (1956) The stratigraphical position of kieslager in the Sambagawa crystalline schist zone in Shikoku. *J. Geol. Soc. Jpn.* **62**, 30–45 (in Japanese with English abstract).

Kunugiza, K. (1984) Metamorphism and origin of ultramafic bodies of the Sanbagawa metamorphic belt in central Shikoku. *J. Mineral. Petrol. Econ. Geol.* **79**, 20–32 (in Japanese).

Kunugiza, K., Takasu, A. and Banno, S. (1986) The origin and metamorphic history of the ultramafic and metagabbro bodies in the Sanbagawa metamorphic belt. *Geol. Soc. Am. Mem.* **164**, 375–385.

Liu, Y. Z. and Tanaka, T. (1999) Osmium-isotopic compositions of Horoman ultramafic complex in Hokkaido, Japan (abstract). *Ninth Ann. V.M. Goldschmidt Conf. LPI Contrib.* **971**, p. 175.

Ludwig, K. R. (2001) Using Isoplot/Ex (v. 2.49): A Geochronological Toolkit for Microsoft Excel. Berkeley Geochronological Center Spec. Pub. 1, Berkeley, 56 pp.

Minamishin, M., Yanagi, T. and Yamaguchi, M. (1979) Rb-Sr whole rock age of the Sanbagawa metamorphic rocks in central Shikoku, Japan. *Isotope Geosciences of Japanese Islands; Report for Scientific Research from the MEJ (No. 334054)* (Yamaguchi, M., ed.), 68–71 (in Japanese).

Miyashiro, A. (1961) Evolution of metamorphic belts. *J. Petrol.* **2**, 277–311.

Möller, A., Post, N. J. and Hensen, B. J. (2002) Crustal residence history and garnet Sm-Nd ages of high-grade metamorphic rocks from the Windmill Islands area, East Antarctica. *Int. J. Earth Sci.* **91**, 993–1004.

Mørk, M. B. E. and Mearns, E. W. (1986) Sm-Nd isotopic systematics of a gabbro-eclogite transition. *Lithos* **19**, 255–267.

Niu, Y. (2004) Bulk-rock major and trace element compositions of abyssal peridotites: Implications for mantle melting, melt extraction and post-melting processes beneath Mid-Ocean Ridges. *J. Petrol.* **45**, 2423–2458.

Okamoto, K., Shinjoe, H., Katayama, I., Terada, K., Sano, Y. and Johnson, S. (2004) SHRIMP U-Pb zircon dating of quartz-bearing eclogite from the Sanbagawa Belt, southwest Japan: implications for metamorphic evolution of subducted protolith. *Tera Nova* **16**, 81–89.

Puchtel, I. S., Brügmann, G. E. and Hofmann, A. W. (1999) Precise Re-Os mineral isochron and Pb-Nd-Os isotope systematics of a mafic-ultramafic sill in the 2.0 Ga Onega plateau (Baltic Shield). *Earth Planet. Sci. Lett.* **170**, 447–461.

Reisberg, L. C. and Zindler, A. (1986) Extreme isotopic variations in the upper mantle: evidence from Ronda. *Earth Planet. Sci. Lett.* **81**, 29–45.

Reisberg, L. C., Zindler, A. and Jagoutz, E. (1989) Further Sr and Nd isotopic results from peridotites of the Ronda Ultramafic Complex. *Earth Planet. Sci. Lett.* **96**, 161–180.

Reisberg L. C., Allègre, C. J. and Luck, J. M. (1991) The Re-Os systematics of the Ronda Ultramafic Complex of southern Spain. *Earth Planet. Sci. Lett.* **105**, 196–213.

Reisberg, L. C., Zindler, A., Marcantonio, F., White, W. and Wyman, D. (1993) Os isotope systematics in ocean island basalts. *Earth Planet. Sci. Lett.* **120**, 149–167.

Righter, K., Chesley, J. T., Geist, D. and Ruiz, J. (1998) Behavior of Re during magma fractionation: an example from Volcán Alcedo, Galápagos. *J. Petrol.* **39**, 785–795.

Roy-Barman, M. (1993) Mesure du rapport $^{187}Os/^{188}Os$ dans les basaltes et les peridotites: contribution a la systematique ^{187}Re-^{187}Os dans le manteau. Thesis, Univ. Paris, 7.

Saal, A. E., Takazawa, E., Frey, F. A., Shimizu, N. and Hart, S. R. (2001) Re-Os isotopes in the Horoman peridotite: evidence for refertilization? *J. Petrol.* **42**, 25–37.

Shaw, D. M. (2000) Continuous (Dynamic) melting theory revisited. *The Canadian Mineralogist* **38**, 1041–1063.

Shirey, S. B. and Walker, R. J. (1995) Carius tube digestion for low-blank rhenium-osmium analysis. *Anal. Chem.* **67**, 2136–2141.

Shirey, S. B. and Walker, R. J. (1998) The Re-Os isotope system in cosmochemistry and high-temperature geochemistry. *Annu. Rev. Earth Planet. Sci.* **26**, 423–500.

Smoliar, M. I., Walker, R. J. and Morgan, J. W. (1996) Re-Os ages of group IIA, IIIA, IVA and IVB iron meteorites. *Science* **271**, 1099–1102.

Sugisaki, R., Shimomura, T. and Ando, K. (1977) An automatic X-ray fluorescence method for the analysis of silicate rocks. *J. Geol. Soc. Jpn.* **83**, 725–733 (in Japanese with English abstract).

Takasu, A. (1984a) Prograde and retrograde eclogites in the Sambagawa metamorphic belt, Besshi district, Japan. *J. Petrol.* **25**, 619–643.

Takasu, A. (1984b) Geology and petrology of the Sanbagawa metamorphic belt in the Besshi district, central Shikoku, Japan. Ph.D. Thesis, Kyoto Univ., 174 pp.

Takasu, A. (1989) P-T histories of peridotite and amphibolite tectonic blocks in the Sanbagawa metamorphic belt, Japan. *Geological Society Special Publication* **43**, 533–538.

Takasu, A. and Dallmeyer, R. D. (1990) $^{40}Ar/^{39}Ar$ mineral age constraints for the tectonothermal evolution of the Sambagawa metamorphic belt, central Shikoku, Japan: a Cretaceous accretionary prism. *Tectonophysics* **185**, 111–139.

Takasu, A. and Kohsaka, Y. (1987) Eclogites from the Iratsu epidote amphibolite mass in the Sambagawa metamorphic belt, Besshi district, Japan. *J. Geol. Soc. Jpn.* **93**, 517–520 (in Japanese).

Takazawa, E., Fray, F. A., Shimizu, N. and Obata, M. (1999) Whole rock compositional variations in an upper mantle peridotite (Horoman, Hokkaido, Japan): Are they consistent with a partial melting process? *Geochim. Cosmochim. Acta* **64**, 695–716.

Tanaka, T. and Masuda, A. (1982) The La-Ce geochronometer: a new dating method. *Nature* **300**, 515–518.

Tanaka, T., Kamioka, H. and Yamanaka, K. (1988) A fully automated γ-ray counting and data processing system for

INAA and analysis of rock reference samples. *Bull. Geol. Surv. Jpn.* **39**, 537–557 (in Japanese with English abstract).

Tanaka, T., Togashi, S., Kamioka, H., Amanawa, H., Kagami, H., Hamamoto, T., Yuhara, M., Orihashi, Y., Yoneda, S., Shimizu, H., Kunimaru, T., Takahashi, K., Yanagi, T., Nakano, T., Fujimaki, H., Shinjo, R., Asahara, Y., Tanimizu, M. and Dragusanu, C. (2000) JNdi-1: a neodymium isotopic reference in consistency with LaJolla neodymium. *Chem. Geol.* **168**, 279–281.

Toriumi, M. and Kohsaka, Y. (1995) Cyclic p-t path and plastic deformation of eclogite mass in the Sambagawa metamorphic belt. *Jour. Fac. Sci. Univ. Tokyo Sec. 2* **22**, 211–231.

Wasserburg, G. J., Jacobsen, S. B., DePaolo, D. J., McCulloch, M. T. and Wen, T. (1981) Precise determination of Sm/Nd ratios, Sm and Nd isotopic abundances in standard solutions. *Geochim. Cosmochim. Acta* **45**, 2311–2323.

Yokoyama, K. (1976) Finding of plagioclase-bearing granulite from the Iratsu epidote amphibolite mass in central Shikoku. *J. Geol. Soc. Jpn.* **82**, 549–551.

Yokoyama, K. (1980) Nikubuchi peridotite body in the Sanbagawa metamorphic belt: thermal history of the Al pyroxene-rich suite peridotite body in high pressure metamorphic terrain. *Contrib. Mineral. Petrol.* **73**, 1–13.

Yokoyama, K. and Mori, T. (1975) Spinel-garnet-two pyroxene rock from the Iratsu epidote amphibolite mass, central Shikoku. *J. Geol. Soc. Jpn.* **82**, 29–37.